ARTICLE NO. 79-4117

Flight Experience with a Near-Optimal Attitude Control System

Charles A. Bénet*
Lockheed Missiles and Space Co., Sunnyvale, Calif.

This paper discusses some practical aspects of the flight characteristics of a near-optimal control law applied to the attitude control of a suborbital space vehicle. Because of uncertainties in determining the overall system parameters, no attempt was made toward an exact implementation of the optimal control law. Instead, an approximation of the control algorithm was mechanized about two orthogonal axes of the vehicle, resulting in somewhat longer maneuver times. The flight data showed that, in general, the maneuver times did not exceed the calculated optimal times by more than 20%. For some vehicles, however, significantly poorer performances were encountered. Maneuver times exceeding the optimal times by 50% were recorded. These vehicles were also the ones which exhibited the largest inertial crosscouplings between the two control axes. Based upon this, the product of inertia between control axes should be kept to a minimum, in order to retain the shorter maneuvering time advantage of this near-optimal control configuration.

Introduction

THIS paper discusses the development, implementation, and flight test results of an approximate optimal control system. The control law which is derived here, was applied to the attitude control system of a suborbital spacecraft. The flight sequence consisted of a series of combined velocity and attitude changes, with a single thrusting system providing the velocity increments and the attitude maneuvering capability. Minimizing the maneuver times and the overshoots about the commanded attitudes were the design goals. Since the propulsion system was of a type constantly expending energy, a minimum time control law also meant minimum fuel consumption. Because of the design approximations and depending upon the spacecraft and the maneuver characteristics, the maneuver times were 10 to 50% greater than the theoretical optimal times which would have resulted from a more accurate implementation of the optimal control algorithms. However, for the overall mission, the range improvements were significant enough to warrant the small additional complexity in the attitude control implementation.

Theoretical Background

Optimal control theory has shown that minimum time controls for linear second-order systems are "bang-bang," i.e., the control function switches once and only once between its two extrema. Figure 1 is a phase-plane representation of such a system. The switching locus is constituted by the two branches of a parabola OA and OB corresponding to the two directions of thrust. The switching conditions can easily be derived and are given by the equation:

$$\operatorname{sgn}[\theta]\sqrt{|\theta|} + (1/\sqrt{2a})\dot{\theta} = 0 \tag{1}$$

where a is the maximum available angular acceleration provided by the thrust generator.[1]

A mechanization of this switching law is shown on Fig. 2 where

$$K_{R\theta ME} = (1/\sqrt{2a}) \tag{2}$$

Received Aug. 21, 1978; revision received Feb. 26, 1979.

Index category: Spacecraft Dynamics and Control.

*Systems Test Engineer Specialist. Member AIAA.

With this quadratic control law, thrusting changes direction at the proper time, independently of the initial conditions. The system is in "maximum effort," i.e., accelerating, then decelerating towards its new attitude, the exact period of each phase depending upon the initial conditions relative to the switching locus. The saturation block is the engineering realization of the signum operation.

Control Law Implementation

Armed with the knowledge of the optimal control law, we will now discuss the implementation of this control algorithm for the attitude control loops of a space vehicle which is required to undergo a series of repositioning maneuvers. Minimizing the maneuvering time from an arbitrary initial state to a specific target state is the design goal.

The same control law is mechanized about two orthogonal axes (α and β). Four pairs of thrusters, located on these axes, are used to effect clockwise and counterclockwise rotations of the vehicle. Because of uncertainties in determining the system parameters (inertia, thrust lags, delays, etc.), an exact calculation of the ideal switching function is not attempted here. Moreover, for practical reasons, the approximation of the control algorithm makes use of the sine of the attitude command θ which is provided to the attitude control microprocessor by the guidance subsystem computer.

Figure 3 is a block diagram of the approximate optimal attitude control system. The square root of the attitude command θ is approximated as $\text{sine}\theta + 0.2$. The rationale for this approximation is made clear by simple examination of Fig. 4.

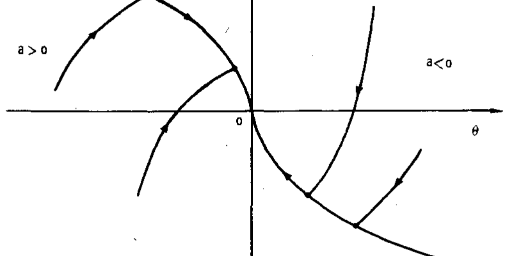

Fig. 1 Response of a time-optimal control system.

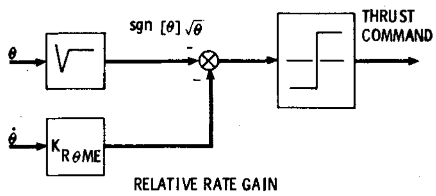

Fig. 2 Block diagram of a time-optimal control system.

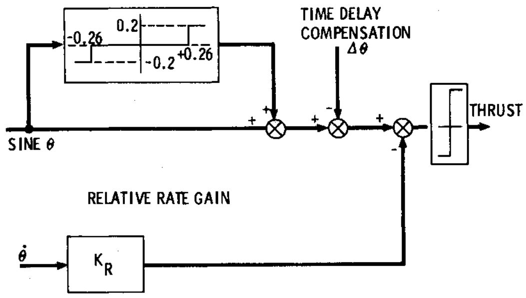

Fig. 3 Implementation of an approximate "max. effort" control system.

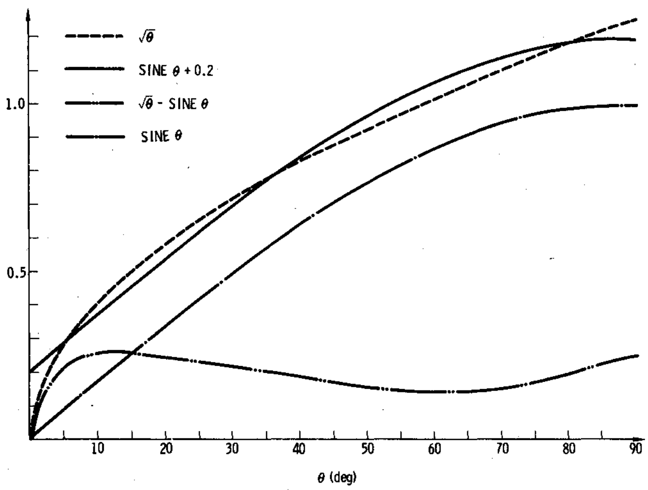

Fig. 4 Square root approximation for the attitude command.

Since switching of the thrust direction will now occur for dynamic conditions other than the ones corresponding to the exact switching curve, limit cycling, overshoots, and chattering about the switching can be generated. To prevent these detrimental effects, the system is designed to revert to a proportional attitude path as soon as the vehicle is within 15 deg of its commanded attitude. For this region the system is simply an attitude control system with a rate feedback loop ($\sin\theta \sim \theta$). The control thrusters are then time modulated, resulting in an average thrust proportional to the attitude error. This dual mode of operation combines many of the advantages of both linear and optimum control systems.[2]

System Parameters Determination

Relative Rate Gain K_R

The relative rate gain K_R is being switched between the "max. effort" rate gain $K_{R\theta ME}$ and the linear rate gain $K_{R\theta}$. For an ideal system, $K_{R\theta ME}$ is determined from the switching locus equation, $K_{R\theta ME} = 1/\sqrt{2a}$ where a is the system's maximum acceleration capability. $K_{R\theta}$, the linear rate gain value, is determined by classical control theory considerations of stability and response characteristics. A phase margin greater than 30 deg and a gain margin in excess of 6 dB were used as design criteria of the linear region of operation.

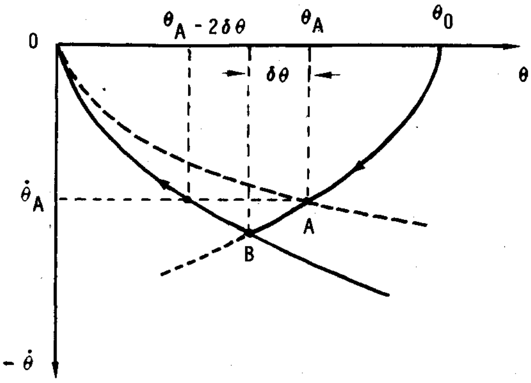

Fig. 5 Switching time compensation for system delays.

Time Delay Compensation

The system time delays require compensation. For an ideal system without delays, switching command and actual switching occur at point B (Fig. 5). However, because of the response time inherent to the physical system, the switching command to achieve actual switching at point B must be given somewhat earlier, at point A for instance.

The new switching condition, that is the equation of the new sitching locus OA, can be written by inspection of Fig. 5. Let's assume that we are dealing with a time delay t_d.

If θ_A and $\dot{\theta}_A$ are the coordinates of point A,

$$\delta\theta = \dot{\theta}_A t_d + \tfrac{1}{2} a t_d^2 \tag{3}$$

At point B of the old switching locus we have

$$\theta_A - 2\delta\theta = \dot{\theta}_A / 2a \tag{4}$$

Replacing by its value in Eq. (3) in Eq. (4) yields

$$\theta_A - 2\dot{\theta}_A t_d - a t_d^2 = \dot{\theta}_A^2 / 2a \tag{5}$$

or

$$\theta_A = (1/2a)\,[\dot{\theta}_A^2 + 4a\dot{\theta}_A t_d + 2a^2 t_d^2] \tag{6}$$

$$= (1/2a)\,[(\dot{\theta}_A + 2at_d)^2 - 2a^2 t_d^2] \tag{7}$$

Neglecting $2a^2 t_d^2$ the new swtiching criterion becomes

$$\mathrm{sgn}\sqrt{\theta_A} + (1/\sqrt{2a})\dot{\theta}_A + \sqrt{2a}t_d = 0 \tag{8}$$

We recognize the factor $1/\sqrt{2a}$ which is the relative rate gain $K_{R\theta ME}$, previously defined. The term $\sqrt{2a}t_d$ is the time delay compensation and is labeled $\Delta\theta$ in Fig. 3. $\Delta\theta$ is a function of the system time delay and of the vehicle acceleration capability. It is set to zero for the linear portion of the control law, the time delay for this mode of operation being accounted for in the loop parameters.

Preflight System Simulation

Extensive preflight system simulations were performed. The effects of spacecraft characteristics (inertial crosscoupling between axes), maneuver amplitudes and distributions between axes (as defined by the angle ψ on Fig. 7) were investigated. A computerized iterative process was used to optimize the system parameters, i.e., $K_{R\theta ME}$ and $\Delta\theta$. Two $[K_{R\theta ME}, \Delta\theta]$ pairs would normally be required since the vehicle moments of inertia about α and β axes are not necessarily identical. To keep the implementation of the design manageable, only one pair of parameters was selected, with only a slight additional deterioration of the optimal law.

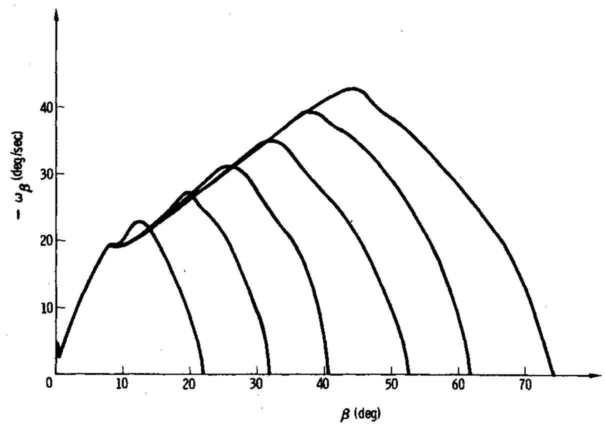

Fig. 6 Phase-plane representation of a simulated maneuver.

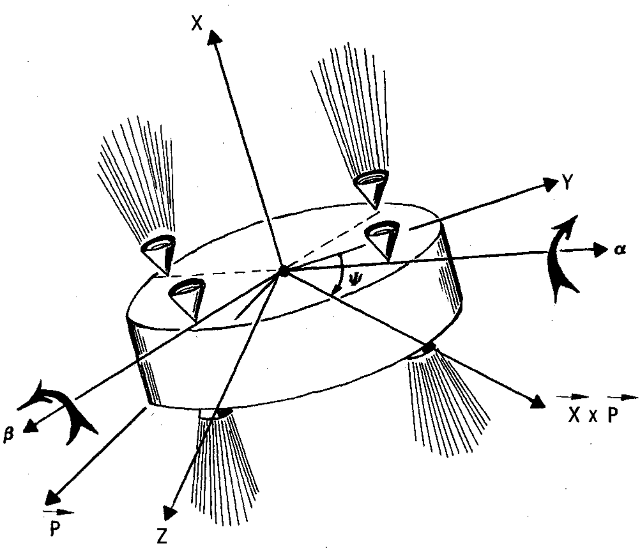

Fig. 7 Sketch of the flight article.

Moreover, because of the approximations made to the optimal law, the system was not completely insensitive to initial conditions, requiring that the system parameters be selected conservatively to minimize overshoots and sensitivity to attitude change magnitudes.

Finally, for each mission, the selected $[K_{R\theta ME}, \Delta\theta]$ sets were validated by a series of preflight simulations. The simulations incorporated a detailed modeling of the vehicle dynamics, rate gyros, thrust system characteristics, transition from linear to "max. effort" operations, etc. Figure 6 shows the phase-plane (β axis) representation of a typical computer simulation run.

Flight Test Results

Figure 7 is a sketch representing the flight article. The objective of the attitude control system is to maneuver the space vehicle in order to align the vehicle longitudinal axis X with the guidance pointing vector $\vec{P}$, fixed in the inertial frame of reference. Four pairs of valves are used to control the maneuver. Smaller valves (not shown on the figure) are included to control the vehicle rotation about the X axis. The criterion used to evaluate the performances of this control system is to compare the actual maneuver time recorded in flight with the theoretical maneuver time, $t_{\min.}$ of an ideal optimal system. For each axis, $t_{\min.}$ is given by the relation:

$$t_{\min.} = 2\sqrt{\theta_0 I/T} \tag{9}$$

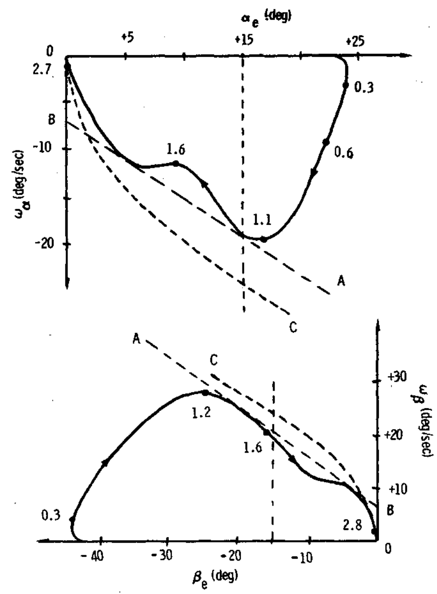

Fig. 8 Phase-plane representation of a maneuver where both control channels are in "max. effort."

where

θ_0 = magnitude of the turn about the axis
I = moment of inertia of the vehicle about the turn axis
T = maximum available torque about the turn axis

In the following discussion, $t_{\min.}$ is calculated by replacing the ratio T/I in Eq. (9) by a, the maximum acceleration recorded during the flight, thus taking into consideration any deviations from nominal values for torque and inertia. Two turn times are calculated $t_{\min.\alpha}$ and $t_{\min.\beta}$, for rotation about the α and β axis, respectively. The greater of the two $t_{\min.}$'s is chosen as representing the optimal maneuver time.

For reasons unrelated to this study, in-flight sensing and telemetering of the vehicle dynamics were made in the XYZ coordinate system instead of the $X\alpha\beta$'s (Fig. 7). The actual maneuver times were defined as the time to bring the spacecraft Y and Z axes within 10 deg of their commanded positions with 5 deg/s residual rates. This criterion was used as a convenient and consistent means of comparing maneuvering times.

From the flight results, the maneuvers were classified in two major categories: 1) both α and β axes entered the "max. effort" region of operation, 2) one axis α and β remained in the linear region of operation. Figure 8 shows the phase-plane representation of an attitude change during which both α and β axes enter the "max. effort" region. Notice the small irregularity in the phase-plane following the passage from the "max. effort" to the linear domain.

Line AB is the approximate switching line represented by the equation

$$\sin\theta + \Delta\theta = K_{R\theta ME}\dot{\theta} \tag{10}$$

Note that in this equation, the constant term 0.2 of the square root of θ approximation is included in $\Delta\theta$. Line OC is the branch of parabola of equation

$$\theta = K^2_{R\theta ME}\dot{\theta}^2 \tag{11}$$

representing the ideal quadratic "max. effort" law. The time (in seconds) from the beginning of the turn is indicated along the curves. Table 1 shows the details of this attitude change. Equation (9) gives the optimal times, $t_{\min.\alpha} = 1.9$ s and $t_{\min.\beta} = 2.45$ s, for the axes α and β, respectively. As listed in

Table 1 Maneuver 1 characteristics

	Units	α	Axis	β
Turn magnitude	deg	23.5		−43.8
Maximum rate	deg/s	−20.0		27.8
Maximum acceleration $\|a\|$	deg/s^2	26.0		29.0
Time to turn (attitude errors and residual rates within 10 deg and 5 deg/s respectively)	s		2.68	
Overshoot	deg	<0.2		<0.2
Time in maximum effort	s	1.00		1.0

Table 2 Maneuver 2 characteristics

	Units	α	Axis	β
Turn magnitude	deg	80		10
Maximum rate	deg/s	−50		−14
Maximum acceleration $\|a\|$	deg/s^2	39		
Time to turn (attitude errors and residual rates within 10 deg and 5 deg/s, respectively)	s		3.72	
Time in maximum effort	s	2.60		0

Table 1, the actual maneuver time was 2.68 s. This is about 10% greater than $t_{\min,\beta}$.

Table 2 gives the details of a maneuver consisting mostly of a rotation about the α axis. The rotation about the β axis remained in the linear region of the control system. For the α axis in "max. effort," the calculated $t_{\min,\alpha}$ is 2.86 s. The recorded time to turn in flight was 3.72 s, thus exceeding the the theoretical optimal time by about 30%.

Based upon our criterion this second maneuver was obviously less efficient than the first one. Other maneuvers with only one control axis entering the "max. effort" region were investigated. Figure 9 represents one of them, with only the α axis operating in the near optimal region of operation. The efficiency of this maneuver was comparable to the one shown in Fig. 8. Consequently, "imbalance" between control channels, that is, turn configuration in which most of the rotation is about one control axis, was not the only cause for the degradation of the turn maneuver deficiency. To gain additional insight into the response characteristics of the vehicle, a detailed analysis of the equations of motion became necessary.

Analysis of Inertial Crosscoupling Between Axes

The use of Euler's equations to describe the dynamics of the vehicle gives the following results:

$$T\beta = \dot\omega\beta I_{\beta\beta} + \omega_\alpha\omega_x(I_{xx} - I_{\alpha\alpha}) + I_{\beta\alpha}(\omega_x\omega_\beta - \dot\omega_\alpha) - I_{\beta x}(\dot\omega_x + \omega_\alpha\omega_\beta) - I_{\alpha x}(\omega_\alpha^2 - \omega_x^2) \tag{12}$$

where

I_{ii} = moment of inertia about the i axis
I_{ij} = product of inertia about the set of axes i, j
ω_i = angular rate about axis i
T_i = sum of the external torques about the i axis

(Refer to Fig. 7 for a description of the system of coordinates.) Rotation rate about the X axis (roll) is usually small, thus the preceding equation can be reduced to

$$T_\beta = \dot\omega_\beta I_{\beta\beta} - I_{\beta\alpha}\dot\omega_\alpha - I_{\beta x}\omega_\alpha\omega_\beta - I_{\alpha x}\omega_\alpha^2 \tag{13}$$

$$= M_{\alpha\beta} + \dot\omega_\beta I_{\beta\beta} - I_{\beta x}\omega_\alpha\omega_\beta \tag{14}$$

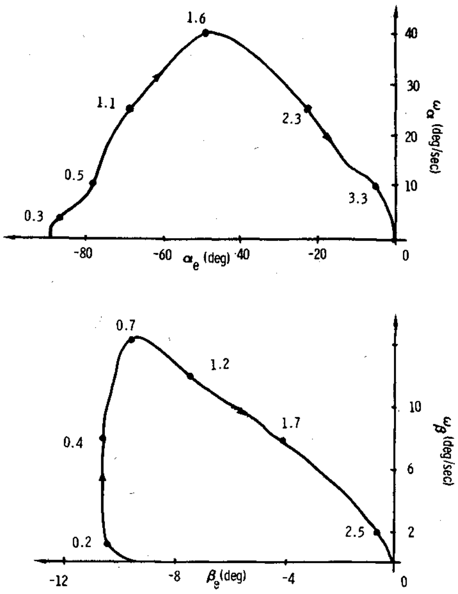

Fig. 9 Phase-plane representation of a maneuver with α channel in "max. effort" and β channel remaining linear.

where

$$M_{\alpha\beta} = -I_{\beta\alpha}\dot\omega_\alpha - I_{\alpha x}\omega_\alpha^2 \tag{15}$$

is the moment coupled from the α axis into the β axis.

The turns represented by Table 2 and Fig. 9 are characteristic of two extremes in inertially crosscoupled torques. For the maneuver of Table 2, $M_{\alpha\beta}$ was 10% of the main torque.

In general, it was found that the flight data indicated a direct relationship between the magnitude of the crosscoupled torques and the lengthening of the maneuvering times. Maneuvers for which the crosscoupled torques were less than 1% of the main torques were quite efficient, exhibiting turn times exceeding the optimum times by only 10-20%. On the other hand, for higher crosscoupled torques (10% or more of the main torques), the turn times exceeded the corresponding optimal times by as much as 50%.

Conclusion

This attitude control system design has shown one practical method of approximating an optimal control law. The flight tests showed that the major contributor to the performance degradation of this approximate optimal design was the dynamic crosscoupling between the two orthogonal control axes about which the control algorithm was mechanized. For small crosscoupling torques, the two control channels remained practically independent and the turn times exceeded the optimal times by no more than 20%.

When the inertially crosscoupled torques between axes were as high as 10% of the controlling torques, however, the turn times exceeded the optimum times by up to 50%. This was especially noticeable for maneuvers in which only one axis entered the "max. effort" control region, the other control channel remaining within the linear domain of operation.

Acknowledgments

This work was supported by U.S. Navy Contract No. N0003074C0100. The system was developed by the Guidance and Control Department of Lockheed Missiles and Space Co., Sunnyvale, Calif. The author is grateful to the designers, particularly to J.N. Gerberg and C.S. Scarborough, for their information on the control law implementation.

References

[1] Kirk, D.E., *Optimal Control Theory*, Prentice-Hall Inc., Englewood Cliffs, N.J., 1970, pp. 248-259.

[2] Gibson, J.E., *Nonlinear Automatic Control*, McGraw-Hill Book Co., New York, 1963, pp. 439-459.